Weierstraß-Institut
für Angewandte Analysis und Stochastik
Leibniz-Institut im Forschungsverbund Berlin e. V.

Preprint ISSN 2198-5855

Pulse repetition-frequency multiplication in a passively mode-locked semiconductor laser coupled to an external passive cavity

Rostislav M. Arkhipov[1], Andreas Amann[2], Andrei G. Vladimirov[1]

submitted: August 8, 2014

[1] Weierstrass Institute
Mohrenstr. 39
10117 Berlin, Germany
E-Mail: Rostislav.Arkhipov@wias-berlin.de
Andrei.Vladimirov@wias-berlin.de

[2] University College Cork
School of Mathematical Sciences 1.45
Western Gateway Building
Cork, Ireland
E-Mail: a.amann@ucc.ie

No. 1993
Berlin 2014

2010 *Mathematics Subject Classification.* 78A60 78M35 78-05.

2008 *Physics and Astronomy Classification Scheme.* 42.60.Fc 42.55.Px 42.65.Sf 85.30.De.

Key words and phrases. mode-locked lasers, mode-selection, delay differential equations model.

R.M. A. and A.G.V. would like to acknowledge the support of EU FP7 ITN PROPHET, Grant No. 264687. A.G.V. acknowledges the support of the SFB 787 and E.T.S. Walton Visitors Award of the Science Foundation Ireland.

Edited by
Weierstraß-Institut für Angewandte Analysis und Stochastik (WIAS)
Leibniz-Institut im Forschungsverbund Berlin e. V.
Mohrenstraße 39
10117 Berlin
Germany

Fax: +49 30 20372-303
E-Mail: preprint@wias-berlin.de
World Wide Web: http://www.wias-berlin.de/

Abstract

Using a delay differential equation model with two time delays, we investigate the dynamics of a semiconductor laser with an active cavity coupled to an external passive cavity. Our numerical simulations indicate that when the coupling between the two cavities is strong enough and the round-trip time of the active cavity is an integer multiple of the round-trip time of the external passive cavity, a harmonic mode-locking regime can develop in the laser with the pulse repetition period close to the passive cavity round trip time. We also demonstrate that the output field intensity sensitively depends on the relative phase between the electric fields in the two cavities giving rise to a resonant behavior. The period and width of the resonances depend on the ratio of the round-trip times and the coupling between the two cavities. We show that the coupled cavity system under consideration can demonstrate a bistability between different regimes of generation.

1 Introduction

Passively mode-locked semiconductor lasers generate short optical pulses with high repetition rates varying from few to hundreds of GHz. They have important applications in optical telecommunications, sampling, and division multiplexing [1, 2, 3, 4, 5, 6]. Optical spectrum of these lasers is a frequency comb with the line spacing equal to the pulse repetition rate of the mode-locked regime. This repetition rate is limited by the fact that active medium length must be sufficiently large to achieve laser generation as well as by the operational frequencies of the optical modulators [7]. Therefore, different methods for pulse repetition frequency multiplication in such lasers have been used. Among them are the schemes employing colliding pulse mode-locking [8], the group delay dispersion in optical fibers (temporal fractional Talbot effect in optical fibers) [9, 10], chirped fiber Bragg grating based on the same Talbot effect [11, 12], and a number of uniform fiber Bragg gratings [7]. Another method of increasing the pulse repetition rate in a mode-locked laser is based on the use of a Fabry-Perot interferometer as an external spectral filter. This method is attractive due to its simplicity and robustness since commercially available Fabry-Perot filters may be employed [13, 14]. Experimentally it was realized by different authors, see, for example, Ref. [13, 14, 15, 16, 17]. The idea of this method is the following [13]. If the separation between transmission peaks of Fabry-Perot interferometer is exactly m times (m is an integer number) larger than the pulse repetition rate of the laser, then only those laser modes will be transmitted through the Fabry-Perot filter which coincide with the transmission lines of this filter. Since this leads to an increase of the separation between the resulting laser modes by m times, one can expect that the repetition frequency can be increased m times [13]. Typical solid state mode-locked femtosecond lasers have free spectral range from about 100 MHz to 1 GHz [18, 19]. On the other hand, for the precision measurements of astronomical

objects, a comb spacing of 10 to 30 GHz is ideal [19]. This is why filtering of femtosecond-laser frequency combs by an external Fabry-Perot cavity is used to generate a broad spectrum of resolvable lines for astronomical measurements, for instance, in astronomical spectrograph calibration (see reviews [19, 20, 21]).

The problem of mode selection in single section semiconductor lasers is one of the most important problems in the control of laser radiation parameters [22]. In particular, semiconductor lasers with a fixed and predetermined number of primary modes are of interest for a number of applications. For example, two-colour devices are useful for terahertz generation by photomixing [23]. In order to achieve a single mode operation in Fabry-Perot semiconductor lasers different methods have been used. In a distributed feedback laser, a Bragg grating in the active cavity can result in single mode emission [24]. An alternative technique that can modify the lasing spectrum is the incorporation of a number of scattering centers in the form of slots into the laser cavity [25, 26]. This technique enables the design of single mode lasers, two mode lasers, or passively mode-locked discrete mode lasers [27, 28].

Furthermore, systems consisting of optically coupled lasers can exhibit a very rich variety of different dynamical phenomena and have much in common with other nonlinear systems [29, 30, 31, 32, 33]. For example, in optically coupled phase locked lasers the break up of phase-locking can lead to the appearance of chaotic dynamics [31]. The nonlinear dynamics in passively mode-locked semiconductor lasers is actively studied nowadays [34]. In [35, 36, 37, 38, 39] the dynamics of passively mode-locked semiconductor lasers was studied theoretically using a system of delay differential equations model and experimentally. The dynamics of optically injected and hybrid mode-locked semiconductor lasers was considered e.g. in [40, 41].

Optical bistability have been intensively studied for decades because of its potential application to all-optical logic and signal processing, see e.g. [42]. The existence of optical bistability in the system comprising a cavity mode and an ensemble of two-level atoms was demonstrated theoretically in [43]. It was shown that two stable cw regimes may coexist in this system and a hysteresis was observed between these regimes when the frequency of the external harmonic signal was changed. Optical bistability was also studied theoretically and experimentally in optically injected semiconductor lasers [44], semiconductor lasers with optical feedback [45, 46], two coupled semiconductor lasers [47], optically injected two-section semiconductor lasers [48], and other laser systems.

Here using a delay differential equations model we study the dynamics of passively mode-locked semiconductor ring laser coupled to an external passive cavity. The external cavity in this case is used as a filter which suppresses certain longitudinal modes of the passively mode-locked laser. We demonstrate an increase of pulse repetition frequency f_p by a factor of 2 and 3 when the external cavity length is 2 and 3 times smaller than the active cavity. We study the dependence of these regimes on the model parameters and coupling coefficients between the two cavities. We demonstrate that changing the relative phase between the two electric fields in the two cavities leads to a periodic appearance of mode-locking windows with frequencies $2f_p$ and $3f_p$, respectively. The period and width of these mode-locking windows depend on the external cavity length.

Finally we demonstrate the existence of optical bistability between a mode-locked regime and irregular pulsations in the model equations. We have found that a bistable behavior arises when

the relative phase between electric fields in two cavities and the pumping power are changed.

2 Model Equations

Our analysis is based on a set of delay differential equations (DDE) describing time evolution of the electric field amplitudes in the active cavity $A_1(t)$ and in the external cavity $A_2(t)$, as well as the saturable gain $G(t)$, and the saturable absorption $Q(t)$ in the gain and saturable absorber (SA) sections of the active cavity (see Fig. 1). This model is given by:

$$\frac{dA_1}{dt} = -\gamma_1 A_1 + \gamma_1\sqrt{\kappa}\sqrt{\kappa_1}e^{\frac{(1-i\alpha_g)G(t)-(1-i\alpha_q)Q(t)}{2}}A_1(t-T_1)e^{i\psi} + \\ +\gamma_1\sqrt{1-\kappa}\sqrt{\kappa_2}A_2(t-T_2)e^{i\phi}. \quad (1)$$

$$\frac{dA_2}{dt} = -\gamma_2 A_2 + \gamma_2\sqrt{1-\kappa}\sqrt{\kappa_1}e^{\frac{(1-i\alpha_g)G(t)-(1-i\alpha_q)Q(t)}{2}}A_1(t-T_1)e^{i\psi} + \\ +\gamma_2\sqrt{\kappa}\sqrt{\kappa_2}A_2(t-T_2)e^{i\phi}. \quad (2)$$

$$\frac{dG}{dt} = g_0 - \gamma_g G - e^{-Q}\left(e^G - 1\right)|A_1(t-T_1)|^2. \quad (3)$$

$$\frac{dQ}{dt} = \gamma_q(q_0 - Q) - s\left(1 - e^{-Q}\right)|A_1(t-T_1)|^2. \quad (4)$$

Here T_1 (T_2) is the round trip time in the active (passive) cavity. The parameters ϕ and ψ describe the phase shifts of the fields A_1 and A_2 after the round trip in the active and passive cavity, respectively. Equations (1)-(4) generalize the model of a passively mode-locked semiconductor laser proposed in [35, 36, 37] to the case of two coupled cavities. The parameters κ, κ_1, and κ_2 describe the reflectivities of the mirrors 3, 2, and 5, respectively, see Fig. 1. Typical values and a short description of the model parameters are given in Table 1. Each of the two coupled cavities has its own spectral filtering element. Since the passive cavity is empty, we assume that the spectral filtering bandwidth is much larger in the passive cavity than in the active one, $\gamma_2 \gg \gamma_1$. Below, for simplicity we will consider the case when $\psi = 0$. The effect of the phase ϕ on the dynamics of coupled cavity laser is studied in Section 5. Let the active cavity round trip time be equal to 25 ps. This corresponds to the pulse repetition frequency close to 40 GHz in the absence of external cavity and to $T_1 = 2.5$ in the normalized units of Eqs. (1)-(4) [37], where the time is normalized to the carrier relaxation time in the absorber section (10 ps).

3 Results of numerical simulations

3.1 80-GHz mode-locking regimes

In this section we present the results of numerical simulations of (1)-(4) with the parameter values given in Table 1. We demonstrate that when the external cavity length is approximately

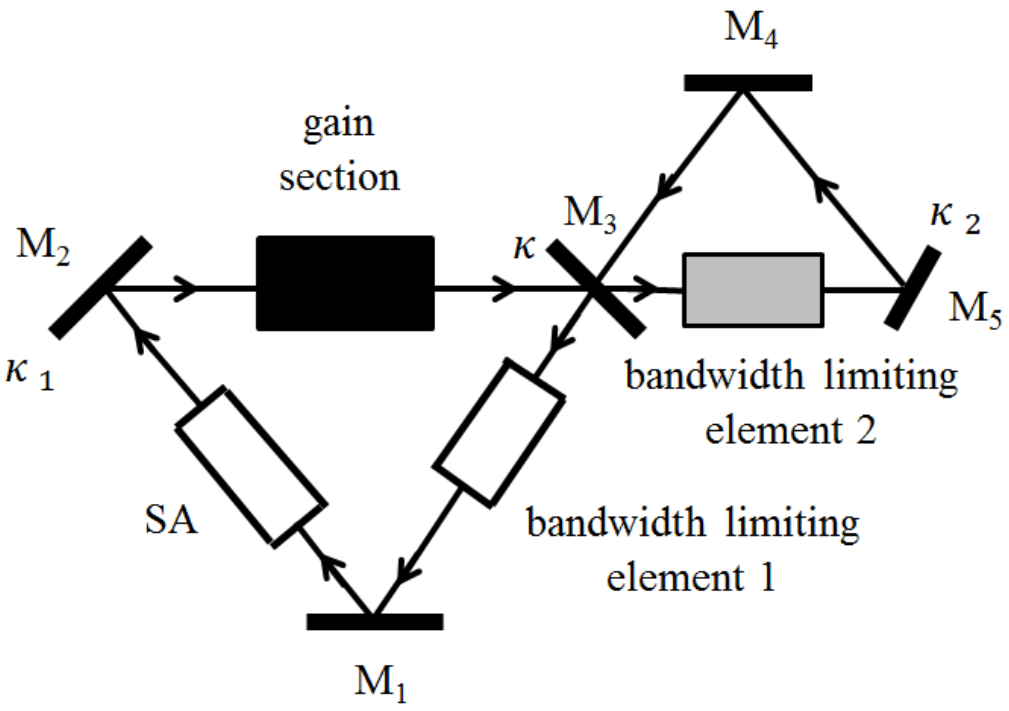

Figure 1: Schematic representation of mode-locked laser coupled to an external passive cavity. The active cavity contains gain section, saturable absorber section, and a spectral filtering element with the bandwidth γ_1. External passive cavity contains only a spectral filtering element the width bandwidth γ_2 which is assumed to be much larger than that of the active cavity, $\gamma_2 \ll \gamma_1$. Parameters κ, κ_1, and κ_2 are the reflectivities of the mirrors M_2, M_3, and M_5, respectively.

Table 1: Typical parameter values used in simulations

spectral filtering bandwidth in the active cavity	γ_1	15
spectral filtering bandwidth in the passive cavity	γ_2	50
non-resonant field intensity attenuation factor per cavity round-trip	$\kappa_1 = \kappa_2$	0.3
linewidth enhancement factor in gain section	α_g	0
linewidth enhancement factor in saturable absorber section	α_q	0
pump parameter	g_0	0.5
unsaturated absorption	q_0	2
carrier relaxation rate in gain section	γ_g	0.01
carrier relaxation rate in saturable absorber section	γ_q	1
ratio of gain and absorber saturation intensities	s	10
optical phase shift in the active cavity	ψ	0
optical phase shift in the passive cavity	ϕ	0
active cavity round trip time	T_1	2.5
passive cavity round trip time	T_2	$T_1/2, T_1/3$

twice smaller than the laser cavity length, $T_2 \approx T_1/2$, an increase of the pulse repetition frequency by a factor of 2 can be achieved. First, we study the evolution of dynamical regimes with the increase of the reflectivity κ of the mirror 3. The bifurcation diagram in Fig. 2 shows the laser pulse peak intensity as a function of κ. To calculate this diagram we have used the following procedure. First, Eqs. (1)-(4) have been integrated from $t = 0$ to $t = 5000$ in order to skip the transient behavior. Next, during the time interval from $t = 5000$ to $t = 7000$, the maxima of the intensity time trace $|A_1(t)|^2$ have been plotted for each given value of the parameter κ.

In Fig. 3 four different examples of the laser intensity time trace are given. When the reflectivity κ is small (strong coupling) the laser operates in a cw regime with the electric field intensity independent of time. The intensity time trace illustrating this regime is shown in Fig. 3a. This regime is indicated as CW in Fig. 2. An increase of κ leads to the appearance a harmonic mode-locking regime (ML_2) with the pulse repetition frequency close to 80 GHz (see Fig. 3b). In this regime the laser emits two pulses per active cavity round trip time T_1. The peak intensity of these pulses increases with κ for $\kappa \leq 0.5$. Further increase of the reflectivity κ up to 0.8 leads to a decrease of the pulse peak intensity. When κ becomes larger than 0.8 a transition to a regime ML_{2a} with two pulses in the cavity having different peak intensities takes place via period doubling bifurcation (Figs. 3c). One of these pulses has larger pulse peak power and the other-smaller than the peak power of the harmonic mode-locking regime with two identical pulses shown in Fig. 3b. Finally, at large coupling strengths $\kappa = 1$ the laser undergoes a transition to fundamental mode-locking regime with the repetition frequency 38.88 GHz, see Fig. 3d.

Fig. 4 has been obtained in a similar way to Fig. 2, but with the linear gain g_0 taken as a bifurcation parameter instead of κ. As it is seen from Fig. 4, when the linear gain g_0 is small enough, the laser exhibits a Q-switching regime QS with the laser intensity oscillating at a low frequency (2 GHz), which is approximately one order of magnitude smaller than the pulse repetition frequency f_p of the fundamental mode-locking regime. The corresponding time trace and power

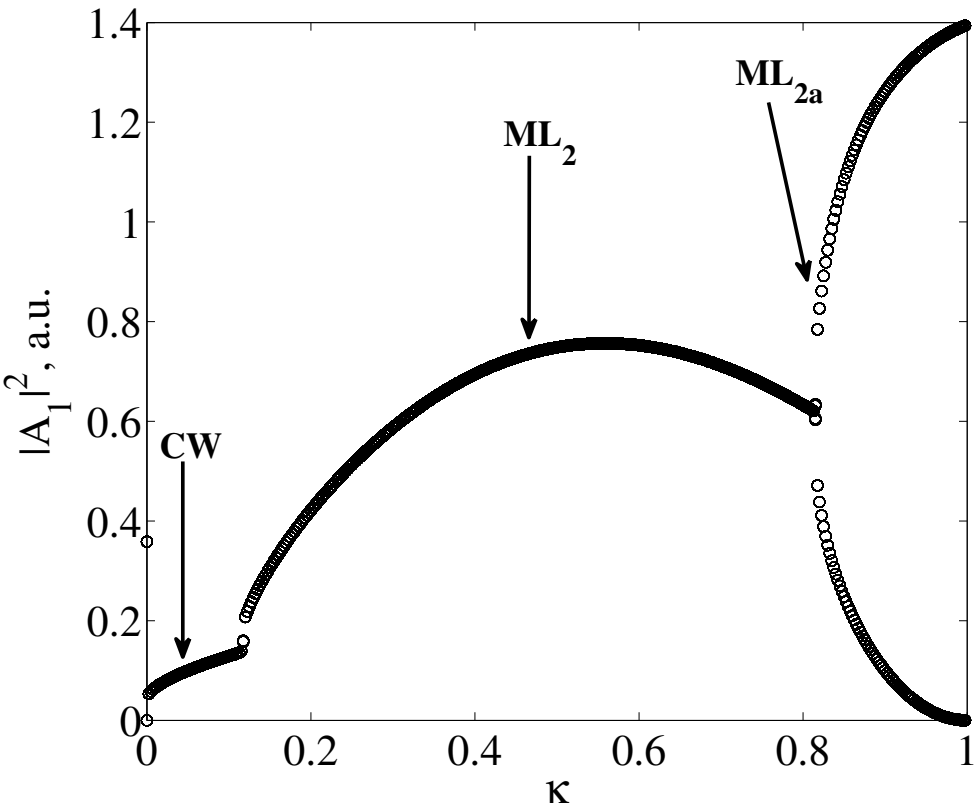

Figure 2: Bifurcation diagram presenting the sequence of dynamical regimes taking place with the increase of the reflectivity κ. $T_2 = T_1/2$, other parameter values are given in Table 1. CW, ML_2, and ML_{2a} indicate continuous wave, 80 GHz mode-locking regime, and 80 GHz mode-locking regime with 2 pulses in the cavity having different peak powers, respectively.

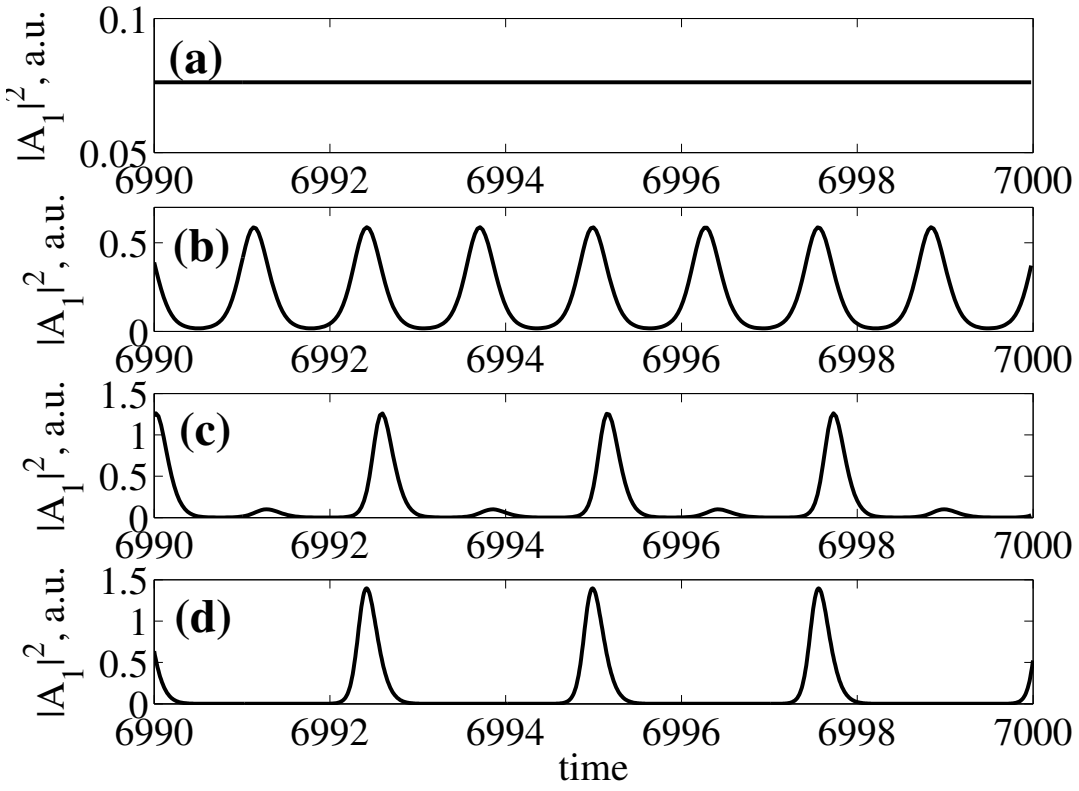

Figure 3: Intensity time traces at different values of the reflectivity parameter κ. (a): CW regime, $\kappa = 0.02$, (b): 80 GHz mode-locking ML_2, $\kappa = 0.3$, (c): harmonic mode-locking regime with two pulses having different peak powers ML_{2a}, $\kappa = 0.9$, (d): 40-GHz fundamental ML regime, $\kappa = 1$.

spectrum are presented in Fig. 5. Q-switching regimes in passively mode-locked quantum dot lasers were studied theoretically in [39]. For the values of the parameter g_0 within the interval (0.161,0.361) the laser operates in a cw regime. With further increase in the pump parameter g_0, a transition to a harmonic mode-locking regime with approximately twice higher repetition rate takes place as shown in Fig. 3b. Finally, for large $g_0 > 1.5$ a cw regime stabilizes once again.

3.2 120-GHz mode-locking regimes

In this subsection we study the dynamics of a passively mode-locked semiconductor laser coupled to an external cavity of length $L/3$, where L is the active cavity length ($T_2 = T_1/3$). In the simulations we have used the parameter values $q_0 = 3$, $\kappa_1 = 0.3$, and $\kappa_2 = 0.9$. Other parameter values are given in Table 1. Similarly to the case in the previous section, when the coupling strength κ is large enough one can expect the appearance of harmonic mode-locking regime with "multiplied" pulse repetition frequency $3f_p$. Such regimes were observed in numerical simulations of a model of passively mode-locked semiconductor laser without external cavity

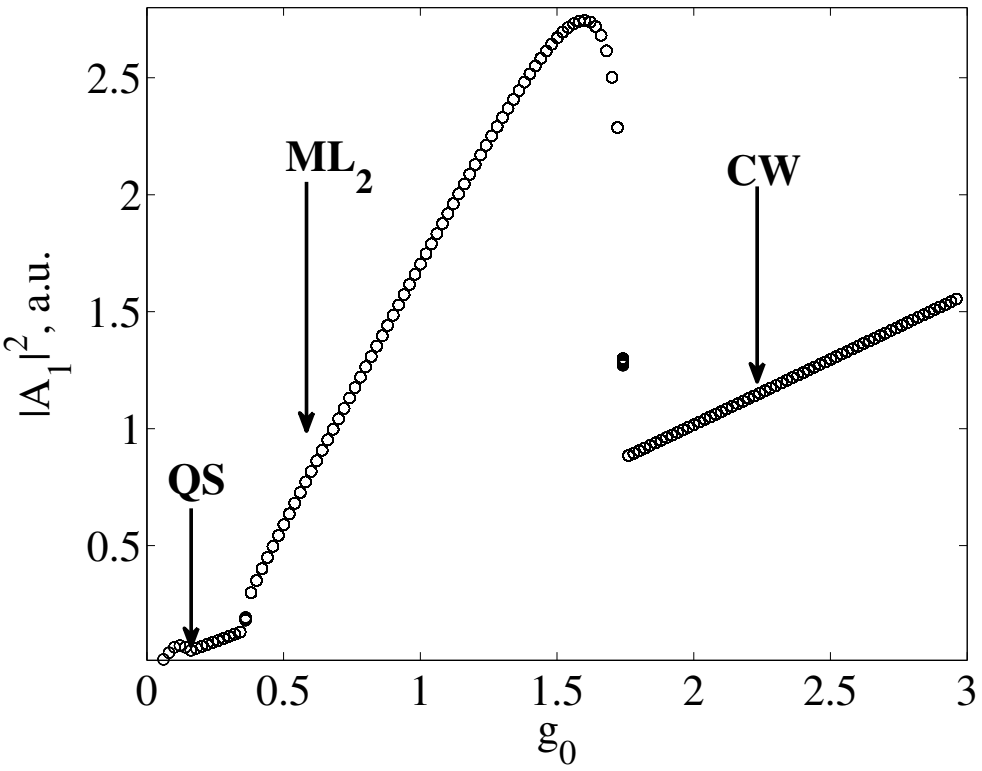

Figure 4: Pulse peak power $|A_1|^2$ versus g_0, $\kappa = 0.3$, $T_2 = T_1/2$. Other parameter values are given in Table 1. Q-switching regime shown in Fig. 5 is indicated as QS.

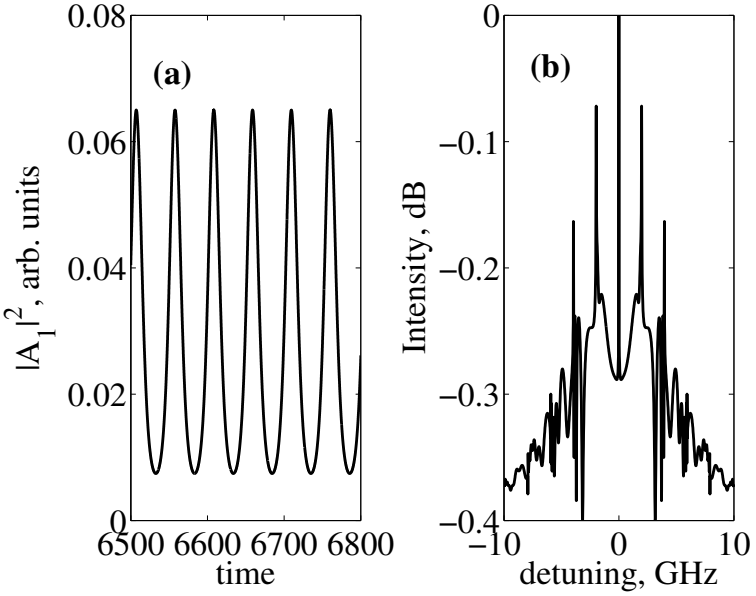

Figure 5: Laser intensity time traces for $g_0 = 0.1$, and $\kappa = 0.3$ (a). Power spectrum (b). Other parameter values are the same as in Fig. 4.

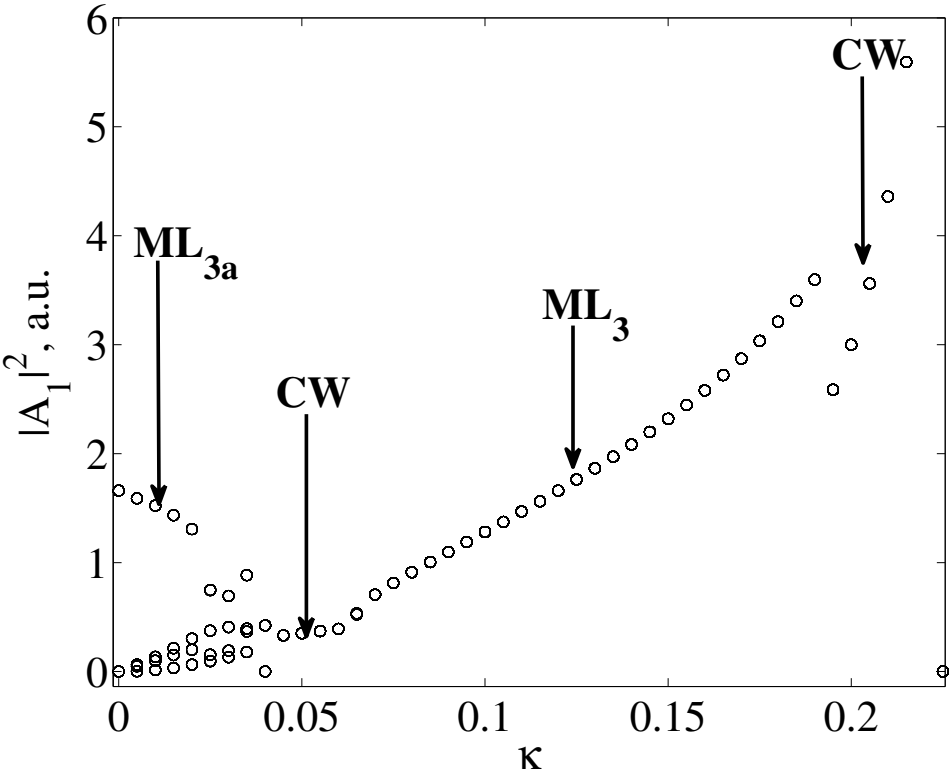

Figure 6: Bifurcation diagram illustrating pulse peak power $|A_1|^2$ as a function of reflectivity κ, $T_2 = T_1/3$, $q_0 = 3$, $\kappa_1 = 0.3$, and $\kappa_2 = 0.9$. Other parameter values are given in Table 1. Mode-locking regimes with three pulses in the cavity having different peak powers are indicated ML_{3a}. Intensity time trace of this regime is shown in Figs. 6a,b. ML_3 indicates harmonic mode-locking regime with the pulse repetition rate 120 GHz, see Fig. 6d.

($\kappa = 1$) at sufficiently large values of the pumping parameter g_0 [37].

Bifurcation diagram illustrating the dependence of the pulse peak power $|A_1|^2$ on the reflectivity κ is presented in Fig. 6. When $\kappa \lessapprox 0.05$ the laser exhibits periodic pulsations (ML_{3a}) with the period close to $2T_1/3$ determined by the sum of the length of the two cavities. Two intensity time traces of this regime corresponding to $\kappa = 0.01$ and $\kappa = 0.03$ are plotted in in Figs. 7a,b. At slightly larger reflectivities the laser starts to operate in CW regime (see Fig. 7c). When κ becomes close to 0.07 harmonic mode-locking regime with the "multiplied" pulse repetition frequency close to $3f_p$ appears. The field intensity time trace for this regime is shown in Fig. 7d. Finally, when κ becomes large enough a transition from the harmonic mode-locking regime to a CW regime takes place.

To study the effect of the injection current on the harmonic mode-locking regime with the pulse repetition frequency $3f_p$, in Fig. 8 we present a bifurcation diagram illustrating the dependence of pulse peak power $|A|_1^2$ on the pump parameter g_0. This figure corresponds to the fixed value of the reflectivity $\kappa = 0.15$, for which this regime occurs in Fig. 6. When g_0 is small enough the laser operates in Q-switching (QS) regime (see Fig. 9), which corresponds to a periodic

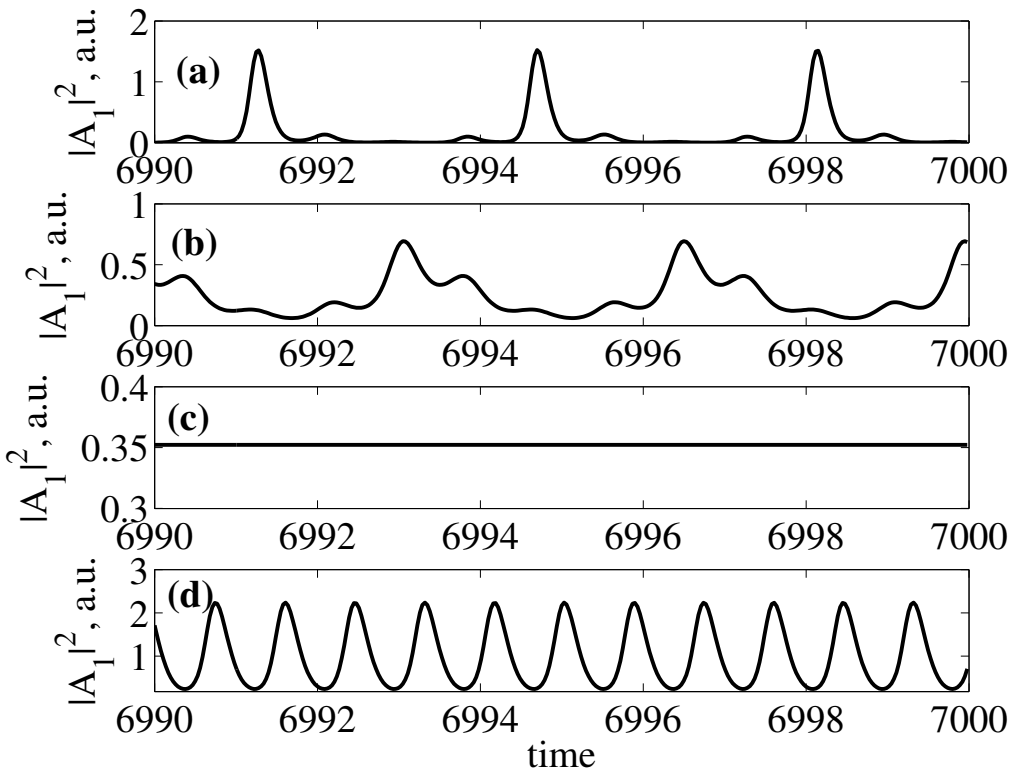

Figure 7: Laser intensity time traces for different values of the reflectivity κ. (a): ML_{3a} regime of periodic pulsations with the period determined by the sum of the round trip times of the two cavities, $2T_1/3$, $\kappa = 0.01$, (b): ML_{3a} regime, $\kappa = 0.03$, (c): CW regime, $\kappa = 0.05$, (d): 120 GHz mode-locking regime ML_3, $\kappa = 0.15$. Other parameter values are the same as in Fig. 6.

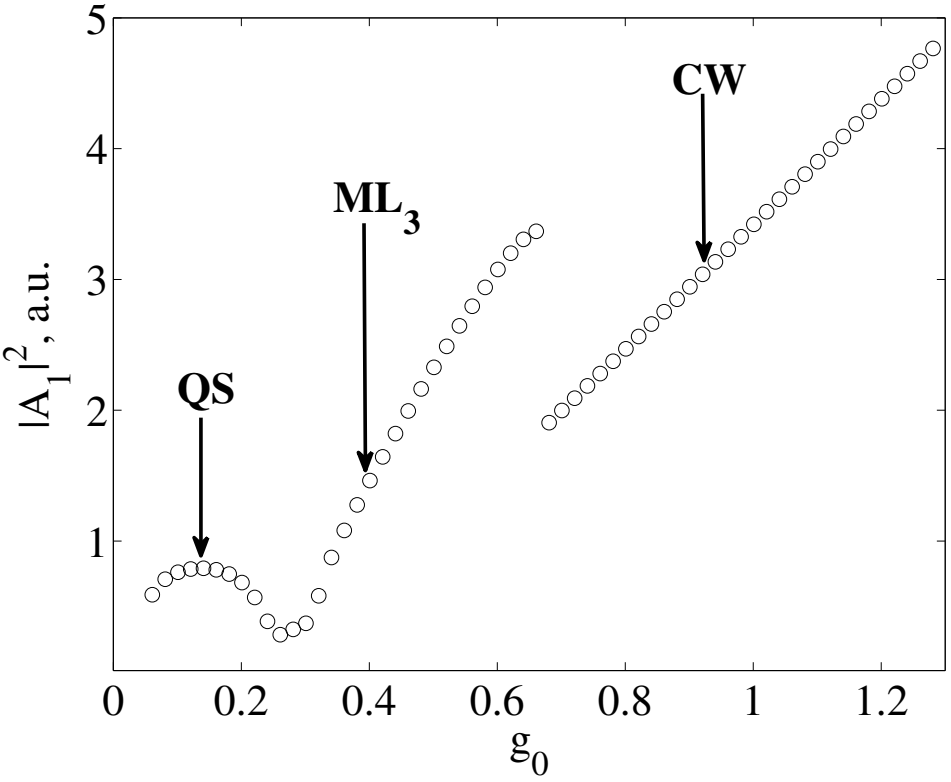

Figure 8: Pulse peak power $|A_1|^2$ versus g_0, $T_2 = T_1/3$, $\kappa = 0.15, \kappa_1 = 0.3$, and $\kappa_2 = 0.9$. Other parameters are the same as in Fig. 6.

pulse train with the pulse peak power oscillating at low frequency close to 1.7 GHz. When g_0 becomes close to 0.3 harmonic mode-locking regime with the pulse repetition frequency close to $3f_p$ (ML_3) appears, as it is seen in Fig. 7d. Finally, for $g_0 > 0.66$ a CW regime becomes stable.

Our analysis indicates that the harmonic mode-locking regimes with the pulse repetition rate $3f_p$ can be observed not only in the case when the external cavity is three times shorter than the active one $T_2 = T_1/3$, but also for $T_2 = 2T_1/3$. In both this cases every third mode of the active cavity coincides with a certain mode of the external passive cavity and, hence, the mode-locking regimes with the pulse repetition rate $3f_p$ can be expected. Bifurcation diagram obtained for the case $T_2 = 2T_1/3$ is similar to that shown in Fig. 6.

4 Nonzero linewidth enhancement factors

In this subsection we study the effect of the linewidth enhancement factors on the dynamics of Eqs. (1)-(4). It is known that at sufficiently large linewidth enhancement factors mode-locking regime can be destabilized leading to the appearance of irregular pulsations. The influence of

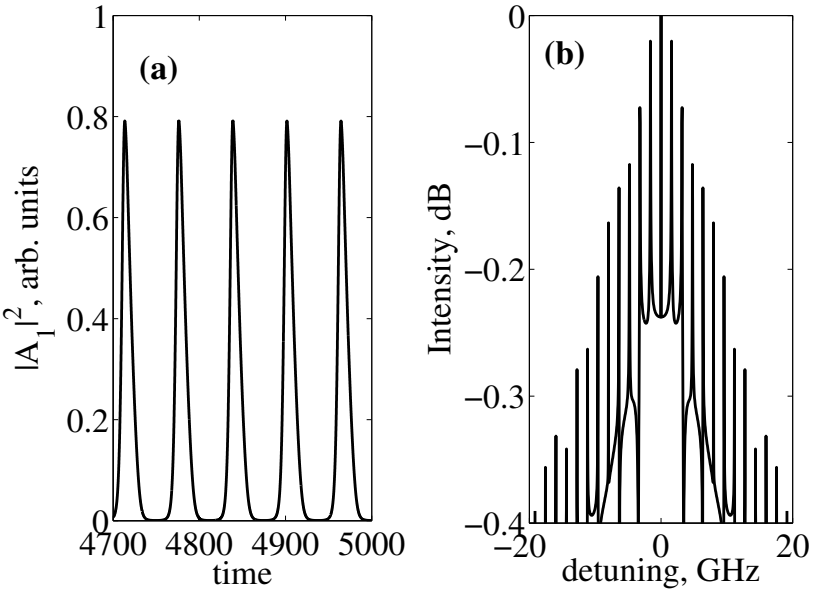

Figure 9: (a): Intensity time traces illustrating Q-switching regime for $g_0 = 0.14$, (b): Spectrum. $T_2 = T_1/3$, $\kappa = 0.15, \kappa_1 = 0.3$, $\kappa_2 = 0.9$. Other parameters are the same as in Fig. 8.

the α-factors on the dynamics of passively mode-locked semiconductor laser without external cavity was studied in [37]. Fig. 10 was obtained by taking the linewidth enhancement factors as bifurcation parameters. It is seen from Fig. 10a corresponding to $\alpha_q = 1.0$ that the largest pulse peak powers were observed in the case when the linewidth enhancement factors in the two sections are approximately equal: $\alpha_g = \alpha_q \simeq 1$. This can be intuitively explained as follows [37]. Since gain and loss enter in equation (1) with opposite signs, the contributions of the gain and absorption sections into the pulse chirp must compensate each other, at least partially, when the two linewidth enchancement factors have the same sign. When α_g is increased the pulse peak power decreases a transition to chaotic and cw regimes takes place (starting from $\alpha_g \simeq 1.7$). Similar behavior was observed for $\alpha_g = \alpha_q$, see Fig. 10b: the pulse peak power decreases with the increase of the two linewidth enhancement factors and a transition to chaotic regime takes place at $\alpha_g = \alpha_q \simeq 3$. It was found in [37] that this transition is associated with the intermittency between mode-locking solution and chaotic intensity pulsations. Slightly above the transition point, time intervals characterized by almost regular mode-locking behavior alternate with irregular spiking. The duration of the "regular"time intervals decreases with the increase of α_g, and, finally, a fully chaotic regime develops. The break up of mode-locking regime can be explained by the presence of intracavity dispersion. When the linewidth enhancement factors are large, frequency separation of the laser modes becomes nonequidistant due to the strong intracavity dispersion, and mode-locking regime disappears.

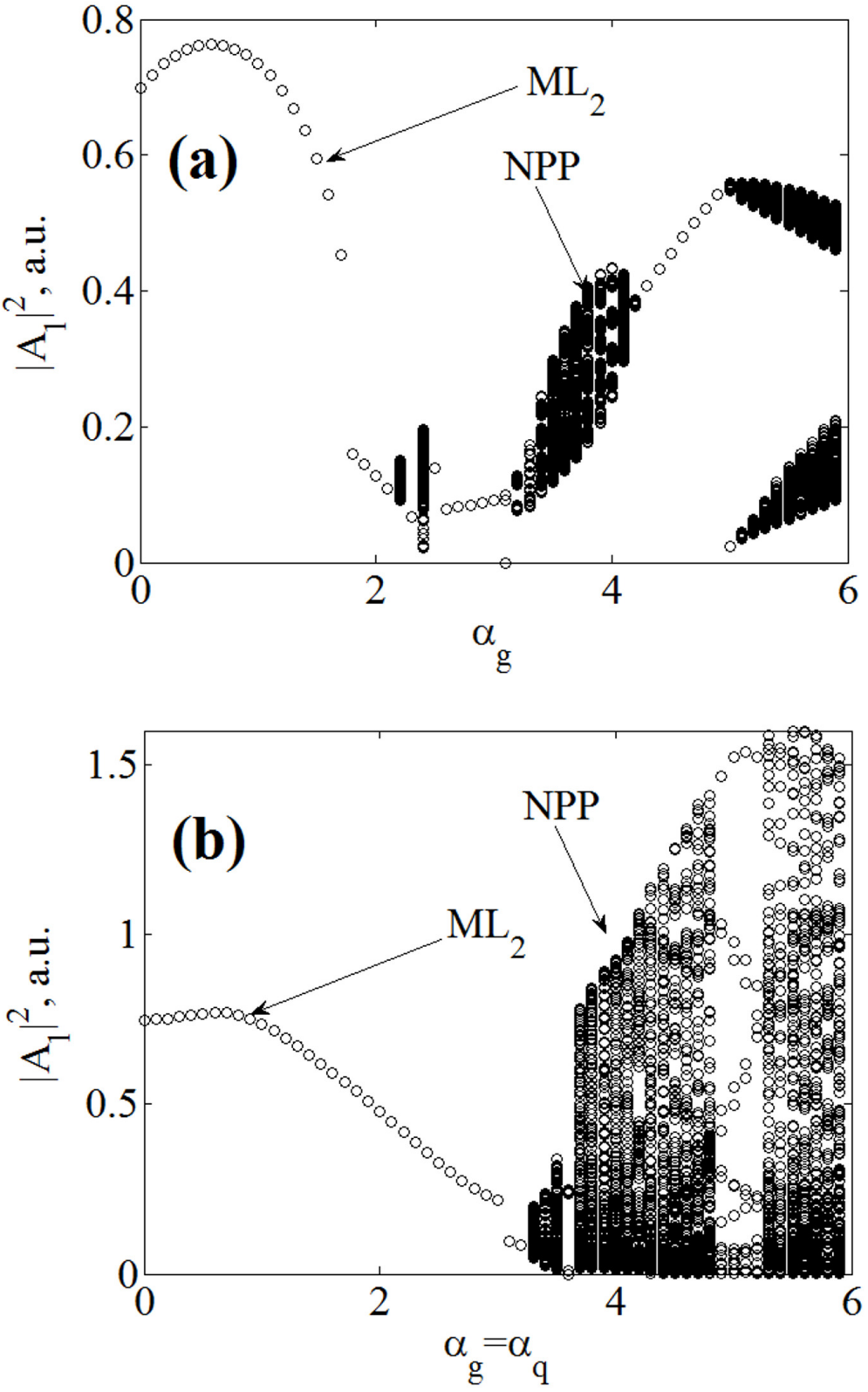

Figure 10: Bifurcation diagrams obtained by changing the linewidth enhancement factors α_g and α_q. $T_2 = T_1/2$. (a) Maxima of the intensity time trace vs α_g, $\alpha_q = 1.0$, (b) Maxima of the intensity time trace vs $\alpha_g = \alpha_q$, $\kappa = 0.5$. Other parameters are given in Table 1.

5 Influence of the relative phase ϕ

In the previous section we assumed that the relative phase between the fields in both cavities is $\phi = 0$. This means that the frequency of the central mode of the active cavity coincides with that of the passive cavity. In order to satisfy this condition it is necessary to make optical length of the external cavity n times smaller than the optical length of the active cavity ($L_2 = L_1/n$, n-integer number) with the precision of a small fraction of a wavelength. However, since in reality it is rather difficult to build the two cavities with such a high precision, it is interesting to consider the dynamics of the coupled cavity laser in the case when the central mode of the passive cavity is shifted in frequency with respect to that of the active cavity, $\phi \neq 0$. To this end we take the phase ϕ as the bifurcation parameter and perform numerical integration of the model equations (1)-(4) with the parameters given in Table 1, $T_2 = T_1/2$, and $\kappa = 0.5$. Bifurcation diagram illustrating the dependence of the pulse peak power $|A_1|^2$ on the parameter ϕ is presented in Fig. 11. It is seen that this dependence has a multi-resonant character and is periodic with the period equal to 2π. This periodicity can be easily understood by taking into account the invariance of equations (1)-(2) under the transformation $\phi \to \phi + 2\pi$. In Fig. 11 the values of ϕ characterized by a single-valued pulse peak power (peak powers of all pulses in the intensity time trace are equal, see Fig. 12a) correspond to mode-locking regimes with the pulse repetition frequency close to $2f_p$. The pulse peak power of this regime achieves its maximum at $\phi = k\pi$ with $k = 0, \pm1, \pm2....$ Finally, near $\phi = (1/2 + k)\pi$ regimes with non-periodic pulsations (NPP) of the pulse peak power are observed. The intensity time traces of these regimes corresponding to a cloud of points in Fig. 11 are shown in Fig. 12b for $\phi = 0.5\pi$.

Resonant behavior similar to that presented in Fig. 11 was observed in the case $T_2 = T_1/3$ as well, see Fig. 13. However, in this case the maximal pulse peak power of the harmonic mode-locking regime at $\phi = k\pi$, $k = 2, \pm4, \pm6...$ and $\phi \approx 0.66k\pi$, $k = 1, \pm2...$ is larger than that in the case $T_2 = T_1/2$ and the windows of non-periodic pulsations are located around $\phi = 0.4\pi, \pi, 1.7\pi$. The nonperiodic NPP regimes appear as a result of destabilization of harmonic mode-locking due to the interference between the electric fields in the two cavities. Note that the resonant behavior shown Fig. 11 is similar to the dependence of the transmission function of a Fabry-Perot cavity on the relative phase ϕ [49].

6 Optical bistability

Bistable devices are important in the field of optical signal processing. They can be used as optical logic elements. In the present section we demonstrate the appearance of optical bistability in the model equations (1)-(4). We consider the case of nonzero linewidth enhancement factors in the gain and absorber sections, $\alpha_g = 3$ and $\alpha_q = 1$. Fig. 14 shows the dependence of the field intensity maxima $|A_1|^2$ on the phase ϕ for $T_2 = T_1/3$. This figure was obtained by numerical integration of the model equations at each value of the parameter ϕ on an equidistant grid with the solution calculated at the previous value of ϕ taken as an initial condition. After the integration the pulse peak intensities were plotted versus the phase ϕ. This procedure was repeated with stepwise increasing and stepwise decreasing of the phase parameter ϕ. Black circles and red crosses in Fig. 14 correspond to the case when parameter ϕ was increased and

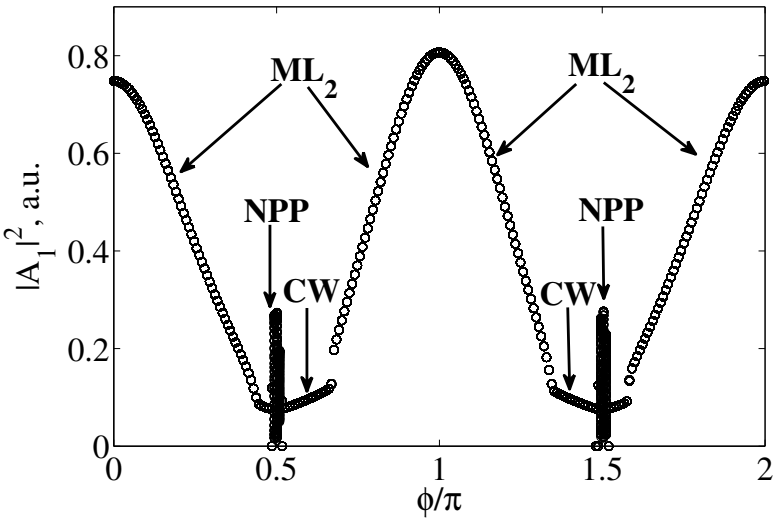

Figure 11: Pulse peak power $|A_1|^2$ versus ϕ. $\kappa = 0.5$, $\kappa_1 = 0.3$, $\kappa_2 = 0.3$, and $T_2 = T_1/2$. Other parameters are given in Table 1. NPP indicates a regime with non-periodic pulsations of the electric field, see Fig. 12b.

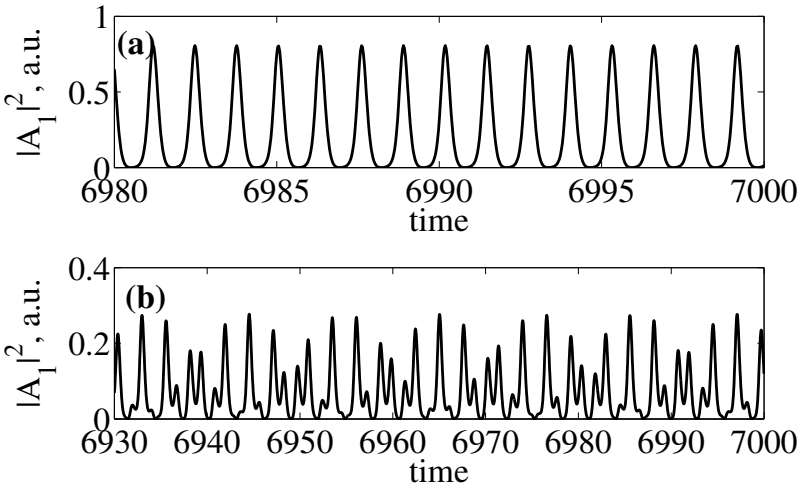

Figure 12: Intensity time traces $|A_1(t)|^2$ calculated for different values of the parameter ϕ. (a): 80 GHz mode-locking, $\phi = \pi$(b): regime of non-periodic pulsations NPP, $\phi = 0.5\pi$. $\kappa_1 = \kappa_2 = 0.3$, $\kappa = 0.5$, and $T_2 = T_1/2$. Other parameter values are given in Table 1.

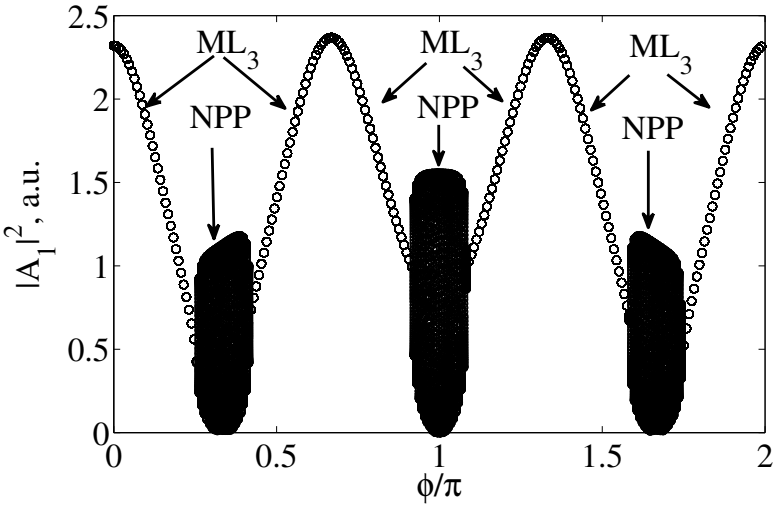

Figure 13: Bifurcation diagram of the pulse peak power $|A_1|^2$ versus ϕ. $\kappa = 0.15$, $\kappa_1 = 0.3$, $\kappa_2 = 0.9$, and $T_2 = T_1/3$). Other parameter values are given in Table 1.

decreased, respectively. It is seen from the figure that within the intervals $0.64\pi \lessapprox \phi \lessapprox 0.74\pi$ and $1.3\pi \lessapprox \phi \lessapprox 1.4\pi$ the laser exhibits a bistability between harmonic mode-locked states (ML_3) with the repetition rate close to 120 GHz and non-periodic regimes (NPP). Furthermore, our simulations demonstrated that the appearance of optical bistability in the system is related to nonzero linewidth enhancement factors in the gain and absorber sections.

In typical experiments on optical bistability the laser output power is measured as a function of the injection current [45, 46, 47]. The diagram shown in Fig. 15 is similar to those in Fig. 4 and Fig. 8, but was obtained with the pump parameter g_0 taken as a bifurcation parameter instead of the detuning ϕ. Fig. 15 was obtained for the case when the external cavity length was three times smaller then that of the active cavity, $T_2 = T_1/3$. It is seen from this figure that when pumping is small the laser operates in Q-switching regime (QS). With the increase of g_0 a transition to harmonic mode-locking regime with the pulse repetition rate close to 120 GHz (ML_{3f}) takes place, see black circles in Fig. 15. Finally, at $g_0 \approx 1.5$ the laser starts to operate in CW regime (CW_f). When the pump parameter is decreased (red crosses in Fig. 15) the laser starts from a CW regime (CW_b in Fig. 15), but the electric field intensity in this case is larger than that of the regime CW_f. The regime CW_b is stable for $g_0 \succeq 0.65$. Below this value a transition to a harmonic mode-locking regime with the frequency close to $3f_p$ (ML_{3b}) takes place. Further decrease of g_0 leads to the transition to Q-switching regime QS coinciding with that obtained by increasing g_0.

Physical reasons of the appearance of bistability can be different. For example, it was demonstrated in Ref.[47] that bistability in 2 coupled semiconductor lasers arises due to the gain saturation that is strongly affected by the mutual coupling of the two cavities.

To demonstrate that the bistability shown in Fig. 15 is related to the presence of the nonzero linewidth enhancement factors in the model equations we integrated these equations with α_g taken as a bifurcation parameter, and $g_0 = 2.98$, see Fig. 16. Red crosses and black circles

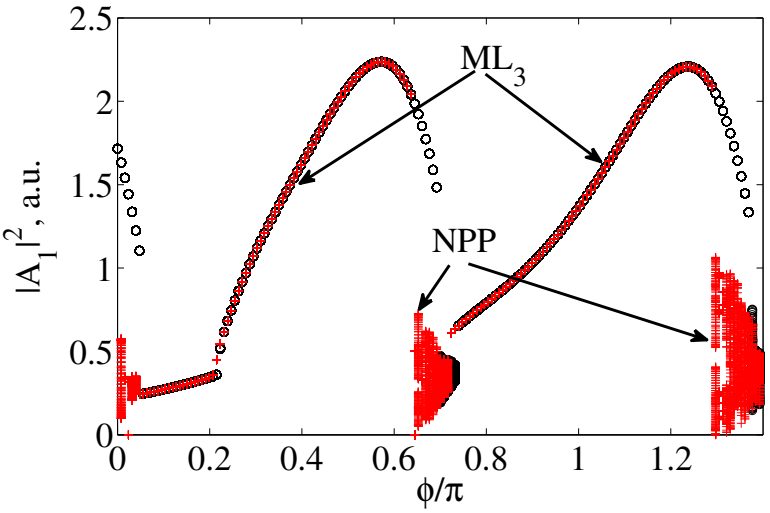

Figure 14: Bifurcation diagram of the pulse peak power $|A_1|^2$ versus ϕ. $q_0 = 3$, $\kappa = 0.15$, $\kappa_1 = 0.3$, $\kappa_2 = 0.9$, $T_2 = T_1/3$, $\alpha_g = 3, \alpha_q = 1$. Black circles (red crosses) correspond to the case when ϕ was increased (decreased). Other parameter values are given in Table 1.

were obtained by decreasing the parameter α_g from $\alpha_g = 3$ to $\alpha_g = 0$ along the branches CW_b and CW_f, respectively, see Fig. 15. The result of these simulations is plotted in Fig. 16. It is seen from Fig. 16 that two stable CW branches coexist for $\alpha_g < \alpha_g^* \approx 0.55$. However, at small $\alpha_g < \alpha_g^*$ the branch CW$_f$ with smaller laser intensity becomes unstable and bistability disappears.

7 Conclusions

In conclusion, we have studied the dynamics of a 40-GHz passively mode-locked semiconductor laser coupled to an external passive cavity. Our analysis was based of a set of delay differential equations governing the time evolution of the electric field envelopes in the two cavities, saturable gain, and saturable absorption. We have shown that the dynamical behavior of the laser depends strongly on the length of the external cavity, the coupling strength between the two cavities, pumping parameter, and the relative phase ϕ. If the length of the external cavity is two or three times smaller than the length of the active cavity and the coupling between two cavities is strong enough, it is possible to generate mode-locking pulses with the "multiplied" repetition frequency close to $2f_p$ or $3f_p$, respectively.

We have investigated the effect of the linewidth enhancement factors on the laser dynamics. In particular, our numerical simulations indicate that at large linewidth enhancement factors mode-locking regimes with the pulse repetition rates $2f_p$ and $3f_p$ can be destroyed and, as a result, a chaotic behavior can develop. Beak up of the mode-locking regimes can be attributed to the intermode distance variation due to the intracavity dispersion.

We have studied the effect of the phase ϕ describing the relative position of the two frequency

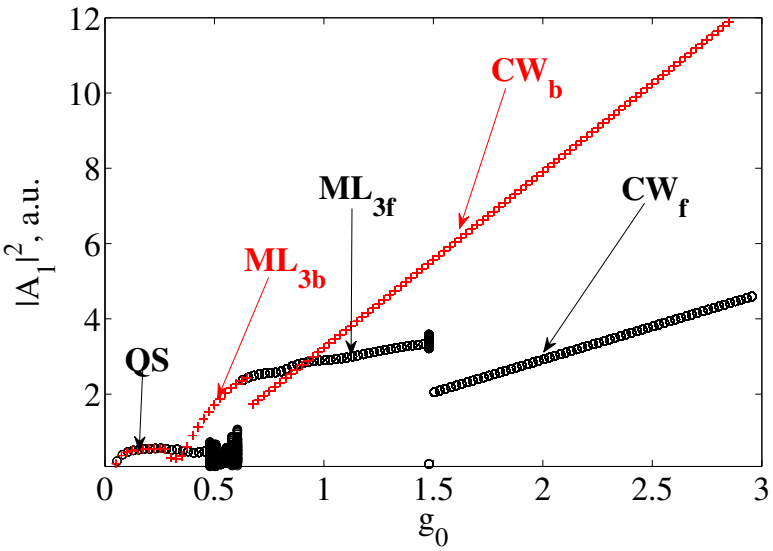

Figure 15: Bifurcation diagram of the pulse peak power $|A_1|^2$ versus pump parameter g_0. $q_0 = 3$, $\kappa = 0.15$, $\kappa_1 = 0.3$,$\kappa_2 = 0.9$, $T_2 = T_1/3$, $\alpha_g = 3, \alpha_q = 1$, and $\phi = 0$. Black circles (red crosses) correspond to the case when g_0 was increased (decreased). Other parameter values are given in Table 1. CW_f and CW_b indicate two bistable CW regimes. ML_{3f} and ML_{3b} correspond to harmonic mode-locking regimes with the pulse repetition frequency close to 120 GHz.

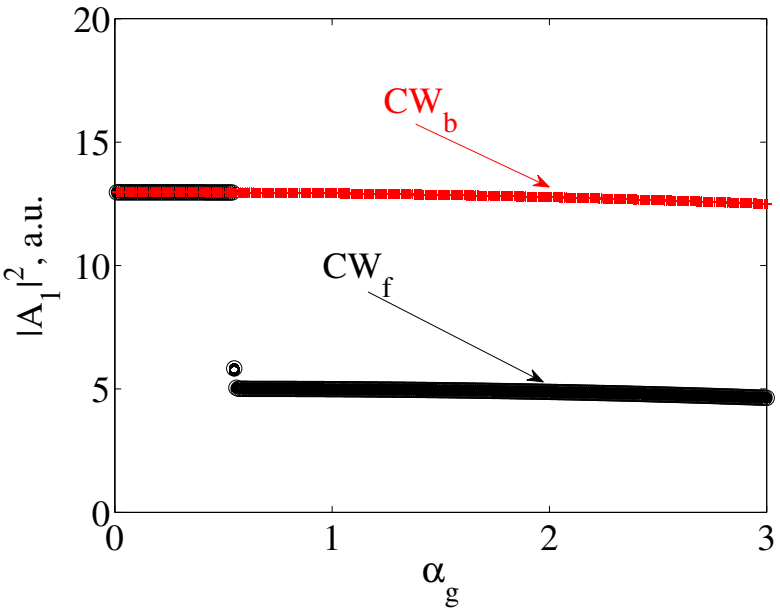

Figure 16: Bifurcation diagram of the pulse peak power $|A_1|^2$ versus α_g. $g_0 = 2.98$. Other parameter values are the same as in Fig. 15.

combs associated with active and passive cavity on the system behavior. Numerical simulations indicate that the pulse peak power has a periodic dependence on ϕ and there is a transition between nonperiodic and mode-locking regimes when ϕ changes. This periodic dependence seems to have the same nature as the dependence of the transmission function of a Fabry-Perot cavity on the electric field phase.

We have demonstrated the existence of optical bistability between different laser operation regimes. The bistability arises when the linewidth enhancement factors are nonzero in the gain and the saturable absorber sections. At zero or sufficiently small linewidth enhacement factors no bistability was observed in our numerical simulations.

Authors are grateful to M. Radziunas and I. Kashchenko for helpful discussions.

References

[1] D. Bimberg, M. Grundmann, N. N. Ledentsov *Quantum dot heterostructures*, vol. 471973882. John Wiley Chichester, 1999.

[2] D. Bimberg, "Quantum dot based nanophotonics and nanoelectronics," *Electronics Letters*, vol. 44, pp. 168–171, 2008.

[3] E. U. Rafailov, M. A. Cataluna, "Mode-locked quantum-dot lasers," *Nature Photonics*, vol. 1, pp. 395–401, 2007.

[4] E. U. Rafailov, M. A. Cataluna, E. A. Avrutin. *Ultrafast lasers based on quantum-dot structures: Physics and devices*, John Wiley & Sons, 2011.

[5] P. G. Kryukov, "Ultrashort-pulse lasers," *Quantum Electronics*, vol. 31, no. 2, pp. 95–119, 2001.

[6] P. G. Kryukov, "Continuous-wave femtosecond lasers," *Physics Uspekhi*, vol. 183, pp. 897–916, 2013.

[7] N. K. Berger, B. Levit, S. Atkins, and B. Fischer, "Repetition-rate multiplication of optical pulses using uniform fiber bragg gratings," *Optics Communications*, vol. 221, no. 4, pp. 331–335, 2003.

[8] R. Fork, B. Greene, and C. Shank, "Generation of optical pulses shorter than 0.1 psec by colliding pulse mode locking," *Applied Physics Letters*, vol. 38, no. 9, pp. 671–672, 1981.

[9] M. H.Takara, S. Kawanishi, "High-repetition-rate optical pulse generation by using chirped optical pulses," *Electronics Letters*, vol. 34, pp. 792–793, 1998.

[10] S. Arahira, S. Kutsuzawa, Y. Matsui, D. Kunimatsu, and Y. Ogawa, "Repetition-frequency multiplication of mode-locked pulses using fiber dispersion," *Journal of Lightwave Technology*, vol. 16, no. 3, pp. 405–410, 1998.

[11] S. Longhi, M. Marano, P. Laporta, O. Svelto, M. Belmonte, B. Agogliati, L. Arcangeli, V. Pruneri, M. Zervas, and M. Ibsen, "40-GHz pulse-train generation at 1.5 μm with a chirped fiber grating as a frequency multiplier," *Optics Letters*, vol. 25, no. 19, pp. 1481–1483, 2000.

[12] J. Azana and M. A. Muriel, "Technique for multiplying the repetition rates of periodic trains of pulses by means of a temporal self-imaging effect in chirped fiber gratings," *Optics Letters*, vol. 24, no. 23, pp. 1672–1674, 1999.

[13] T. Sizer *et al.*, "Increase in laser repetition rate by spectral selection," *IEEE Journal of Quantum Electronics*, vol. 25, no. 1, pp. 97–103, 1989.

[14] K. Yiannopoulos, K. Vyrsokinos, D. Tsiokos, E. Kehayas, N. Pleros, G. Theophilopoulos, T. Houbavlis, G. Guekos, and H. Avramopoulos, "Pulse repetition frequency multiplication with spectral selection in fabry-perot filters," *IEEE Journal of Quantum Electronics*, vol. 40, no. 2, pp. 157–165, 2004.

[15] U. Keller, W. H. Knox, and H. Roskos, "Coupled-cavity resonant passive mode-locked ti: sapphire laser," *Optics Letters*, vol. 15, no. 23, pp. 1377–1379, 1990.

[16] D. K. Serkland, G. D. Bartolini, W. L. Kath, P. Kumar, and A. V. Sahakian, "Rate multiplication of a 59-GHz soliton source at 1550 nm," *Journal of Lightwave Technology*, vol. 16, no. 4, pp. 670–677, 1998.

[17] M. Kirchner, D. Braje, T. Fortier, A. Weiner, L. Hollberg, and S. Diddams, "Generation of 20 ghz, sub-40 fs pulses at 960 nm via repetition-rate multiplication," *Optics Letters*, vol. 34, no. 7, pp. 872–874, 2009.

[18] W. Sibbett, A. Lagatsky, and C. Brown, "The development and application of femtosecond laser systems," *Optics Express*, vol. 20, no. 7, pp. 6989–7001, 2012.

[19] D. Braje, M. Kirchner, S. Osterman, T. Fortier, and S. Diddams, "Astronomical spectrograph calibration with broad-spectrum frequency combs," *The European Physical Journal D*, vol. 48, no. 1, pp. 57–66, 2008.

[20] Z. Jiang, C. B. Huang, D. E. Leaird, and A. M. Weiner, "Optical arbitrary waveform processing of more than 100 spectral comb lines," *Nature Photonics*, vol. 1, no. 8, pp. 463–467, 2007.

[21] T. Steinmetz, T. Wilken, C. Araujo-Hauck, R. Holzwarth, T. W. Hänsch, L. Pasquini, A. Manescau, S. D'Odorico, M. T. Murphy, T. Kentischer, *et al.*, "Laser frequency combs for astronomical observations," *Science*, vol. 321, no. 5894, pp. 1335–1337, 2008.

[22] P. Smith, "Mode selection in lasers," *Proceedings of the IEEE*, vol. 60, no. 4, pp. 422–440, 1972.

[23] M. Tani, O. Morikawa, S. Matsuura, and M. Hangyo, "Generation of terahertz radiation by photomixing with dual-and multiple-mode lasers," *Semiconductor Science and Technology*, vol. 20, no. 7, p. S151, 2005.

[24] L. A. Coldren and S. W. Corsine, *Diode Lasers and Photonic Integrated Circuitss*. New York:Wile, 1995.

[25] B. Corbett and D. McDonald, "Single longitudinal mode ridge waveguide 1.3 μm fabry-perot laser by modal perturbation," *Electronics Letters*, vol. 31, no. 25, pp. 2181–2182, 1995.

[26] S. O'Brien, A. Amann, R. Fehse, S. Osborne, E. P. O'Reilly, and J. M. Rondinelli, "Spectral manipulation in fabry-perot lasers: perturbative inverse scattering approach," *JOSA B*, vol. 23, no. 6, pp. 1046–1056, 2006.

[27] S. Osborne, S. O'Brien, K. Buckley, R. Fehse, A. Amann, J. Patchell, B. Kelly, D. R. Jones, J. O'Gorman, and E. P. O'Reilly, "Design of single-mode and two-color fabry–pérot lasers with patterned refractive index," *IEEE Journal of Selected Topics in Quantum Electronics*, vol. 13, no. 5, pp. 1157–1163, 2007.

[28] S. O'Brien, S. Osborne, D. Bitauld, N. Brandonisio, A. Amann, R. Phelan, B. Kelly, and J. O'Gorman, "Optical synthesis of terahertz and millimeter-wave frequencies with discrete mode diode lasers," *IEEE Transactions on Microwave Theory and Techniques*, vol. 58, no. 11, pp. 3083–3087, 2010.

[29] A. Glova, "Phase locking of optically coupled lasers," *Quantum Electronics*, vol. 33, no. 4, pp. 283–306, 2003.

[30] R. Z. Sagdeev et al., *Nonlinear Physics: from the Pendulum to Turbulence and Chaos*. Chur: Harwood, 2008.

[31] H. Haken, *Laser Light Dynamics*. North-Holland Pub. Co, 1985.

[32] H. E. Hagemeier and S. R. Robinson, "Field properties of multiple coherently combined lasers," *Applied Optics*, vol. 18, no. 3, pp. 270–280, 1979.

[33] M. B. Spencer and W. E. Lamb, "Theory of two coupled lasers," *Physical Review A*, vol. 5, no. 2, p. 893, 1972.

[34] E. Avrutin, J. Marsh, and E. Portnoi, "Monolithic and multi-gigahertz mode-locked semiconductor lasers: Constructions, experiments, models and applications," in *IEE Proceedings-Optoelectronics*, vol. 147, pp. 251–278, IET, 2000.

[35] A. G. Vladimirov and D. Turaev, "A new model for a mode-locked semiconductor laser," *Radiophysics and Quantum Electronics*, vol. 47, no. 10-11, pp. 769–776, 2004.

[36] D. Turaev, G. Kozyreff, *et al.*, "Delay differential equations for mode-locked semiconductor lasers," *Optics Letters*, vol. 29, no. 11, pp. 1221–1223, 2004.

[37] A. G. Vladimirov and D. Turaev, "Model for passive mode locking in semiconductor lasers," *Physical Review A*, vol. 72, no. 3, p. 033808, 2005.

[38] A. G. Vladimirov, A. S. Pimenov, and D. Rachinskii, "Numerical study of dynamical regimes in a monolithic passively mode-locked semiconductor laser," *IEEE Journal of Quantum Electronics*, vol. 45, no. 5, pp. 462–468, 2009.

[39] A. G. Vladimirov, U. Bandelow, G. Fiol, D. Arsenijević, M. Kleinert, D. Bimberg, A. Pimenov, and D. Rachinskii, "Dynamical regimes in a monolithic passively mode-locked quantum dot laser," *JOSA B*, vol. 27, no. 10, pp. 2102–2109, 2010.

[40] N. Rebrova, G. Huyet, D. Rachinskii, and A. G. Vladimirov, "Optically injected mode-locked laser," *Phys. Rev. E*, vol. 83, p. 066202, 2011.

[41] R. Arkhipov, A. Pimenov, M. Radziunas, D. Rachinskii, A. G. Vladimirov, D. Arsenijevic, H. Schmeckebier, and D. Bimberg, "Hybrid mode locking in semiconductor lasers: Simulations, analysis, and experiments," *IEEE Journal of Selected Topics in Quantum Electronics*, vol. 19, no. 4, pp. 1100208–1100208, 2013.

[42] H. Gibbs, *Optical bistability: controlling light with light*. Elsevier, 1985.

[43] A. N. Oraevsky, "Resonant properties of a system comprising a cavity mode and two-level atoms and frequency bistability," *Quantum Electronics*, vol. 29, no. 11, pp. 975–978, 1999.

[44] T. Erneux, E. A. Viktorov, B. Kelleher, D. Goulding, S. Hegarty, and G. Huyet, "Optically injected quantum-dot lasers," *Optics Letters*, vol. 35, no. 7, pp. 937–939, 2010.

[45] P. Glas, R. Müller, and A. Klehr, "Bistability, self-sustained oscillations, and irregular operation of a gaas laser coupled to an external resonator," *Optics Communications*, vol. 47, no. 4, pp. 297–301, 1983.

[46] S. Bauer, O. Brox, J. Kreissl, B. Sartorius, M. Radziunas, J. Sieber, H.-J. Wünsche, and F. Henneberger, "Nonlinear dynamics of semiconductor lasers with active optical feedback," *Physical Review E*, vol. 69, no. 1, p. 016206, 2004.

[47] N. Dutta, G. Agrawal, and M. Focht, "Bistability in coupled cavity semiconductor lasers," *Applied Physics Letters*, vol. 44, no. 1, pp. 30–32, 1984.

[48] A. Pimenov, E. A. Viktorov, S. P. Hegarty, T. Habruseva, G. Huyet, D. Rachinskii, and A. G. Vladimirov, "Bistability and hysteresis in an optically injected two-section semiconductor laser," *Physical Review E*, vol. 89, p. 052903, May 2014.

[49] M. Born, E. Wolf, *Principles of optics*, Pergamon Press, 1980.